Organic & Biomolecular Chemistry

Dynamic Article Links

Cite this: *Org. Biomol. Chem.*, 2011, **9**, 906

www.rsc.org/obc

PAPER

Conformational polymorphism and amphiphilic properties of resorcinarene octapodands†

Kaisa Helttunen,[a] Elisa Nauha,[a] Anni Kurronen,[a] Patrick Shahgaldian[b] and Maija Nissinen*[a]

Received 18th August 2010, Accepted 25th October 2010
DOI: 10.1039/c0ob00602e

o-Nitroaniline functionalized resorcinarene octapodands **1–5** with pendant methyl, ethyl, pentyl, nonyl or 1-decenyl groups, respectively, were synthesized and their structural properties investigated using X-ray crystallography and NMR spectroscopy. The upper rim of each podand is identical containing flexible side arms, in which rotation around the -OCH_2CH_2N- linkers create excellent possibilities for polymorphism. Two conformational polymorphs of acetone solvate of **2** were identified containing different side arm orientation and crystal packing. Compound **1** crystallized from acetone and nitromethane yielding two pseudopolymorphs with different packing motifs. The longer alkyl chains of **3–5** lead to differences in solubility and induce amphiphilic properties, which were studied at the air–water interface using the Langmuir-film technique. Crystals of amphiphilic compound **5**, which has hydrophobic alkyl tails at the lower rim and hydrophilic nitroaniline groups at the upper rim, showed an interesting packing motif with alternating aromatic and aliphatic layers. Versatile structures of the octapodands in solid state and in solution serve as an example of how conformational flexibility can be utilized in crystal engineering and creating self-assembling monolayer structures.

Introduction

Calixarenes and resorcinarenes are widely utilized building blocks for designing supramolecular hosts and self-assembling structures since they offer a concave binding cavity and diverse synthetic pathways for obtaining desired functionalities.[1–6] Recently, work in this field has continued to produce increasingly elaborate host molecules for cations,[7–12] anions,[13,14] ion-pairs,[15,16] neutral guests[10,15,16] and biomolecules.[17,18] In addition, unique self-assembling properties of resorcinarenes have been used to prepare novel nanomaterials with examples ranging from gold/organic microtubular composites[19,20] and coated gold and cobalt nanoparticles[21–24] to dimeric[25,26] and hexameric capsules[27] and molecular containers.[11,12] The design of amphiphilic calixarenes and resorcinarenes bearing long alkyl chains has provided interesting applications,[26,28] such as templating calcite crystallization under monolayers[29] and preparation of solid lipid nanoparticles which interact with DNA[30,31] or proteins.[32]

Resorcinarenes and calixarenes seem to present unlimited possibilities for crystal engineering and creating new supramolecular architectures such as nanotubes,[33,34] preorganizing arrays of fullerene C_{60}[35,36] and benzil in resorcinarene matrices.[37] However, polymorphism, the existence of two or more different crystal forms of one compound, which is considered a very important aspect of crystal engineering,[38] has hardly been studied in these macrocyclic hosts. Resorcinarenes and calixarenes polymorphs have been found by changing crystallization conditions, such as solvent, temperature or pressure,[39–43] but to our knowledge, there are not any reported cases where resorcinarenes or calixarenes are able to form conformational polymorphs[44] in identical crystallization conditions. However, for calixcrowns,[41] a thermally induced conformational change has been reported, and a case of thermal polymorphic change for amino acid derivative of calixarene has been published.[39] Investigation of new polymorphs of a known macrocyclic compound has already provided interesting applications, such as gas absorption in the crystal lattice of various calixarenes.[45–50] In addition, development of new potentially polymorphic compounds can lead the way to new material innovations and deeper understanding of the principles directing the crystallization process.

Our earlier work with tetramethoxy resorcinarenes has provided a selection of cation and anion binding receptors by adding crown ether bridges or pendant groups in upper rim hydroxyl groups.[51–54] A similar synthetic approach has now been applied to resorcinarenes with the objective of creating novel self-assembling properties for supramolecular hosts.

[a]*Department of Chemistry, Nanoscience Center, University of Jyväskylä, P.O. Box 35, FIN-40014, University of Jyväskylä, Finland. E-mail: maija.nissinen@jyu.fi; Fax: +358 14 260 4756; Tel: +358 14 260 4242*
[b]*School of Life Sciences, Institute of Chemistry and Bioanalytics, University of Applied Sciences Northwestern Switzerland, Gründenstrasse 40, 4132, Muttenz, Switzerland*

† Electronic supplementary information (ESI) available: Synthetic procedures and NMR spectra for each podand; details of X-ray structure analysis and crystallographic data. CCDC reference numbers 781919–781925. For ESI and crystallographic data in CIF or other electronic format see DOI: 10.1039/c0ob00602e

Indeed, a selection of structurally flexible resorcinarene octapodands were obtained, which exhibit conformational polymorphism and in the case of long alkyl chain compounds, amphiphilic properties, which were demonstrated by preparing Langmuir-films at the air–water interface, as well as formation of a crystal structure with alternating aromatic and aliphatic layers.

Results and Discussion

Synthesis

Octapodands **3–5** bearing long alkyl chains were prepared by attaching eight *o*-nitro-*N*-(2-hydroxyethyl)aniline units into a resorcinarene platform using Cs_2CO_3 or K_2CO_3 as a base and dibenzo-18-crown-6 as a phase transfer catalyst in refluxing acetonitrile (Scheme 1).[54] The octapodands were obtained as yellow amorphous powders with 40–65% yields. Instead of the tosyl leaving group (compound **6**), a mesyl group (compound **7**) can be used in the reaction as was discovered in the synthesis of **3** and **5**. TG/DTA analysis of **5** showed gradual decomposition between 273–600 °C without a clear melting point according to the enthalpy values. Melting point measurements of each synthesis batch varied between 56 and 77 °C and therefore the reported melting points for amorphous podands should be considered as rough estimates only.

1 and **2** with pendant methyl and ethyl groups, respectively, were synthesized using the above mentioned reaction conditions, but the product was collected from the filtered reaction mixture by extraction with CH_2Cl_2 unlike **3–5**, which are soluble in acetonitrile and were collected from the filtrate. In addition, **1** and **2** were recrystallized from hot acetone to provide orange crystalline solids at 23–31% yield or alternatively treated as the long chain podands to produce amorphous powders at 44–54% yield.‡

Single crystal X-ray crystallography

The octapodands **1**, **2** and **5** provided single crystals suitable for X-ray analysis from nitromethane–CH_2Cl_2 solution (structures **1A**, **2C** and **5A** respectively). Crystallization from nitromethane was a slow process, and took several months for all the investigated compounds providing a selection of yellow needles, blocks, plates and rods. **1A** and **5A** were crystallized without nitromethane in the lattice but **2C**, using acetone solvate as a starting material incorporated two disordered nitromethane molecules per unit cell. Structure **2D**, which crystallized from acetonitrile–CH_2Cl_2 solution has an isomorphous unit cell and packing with **2C**. Compounds **1** and **2** crystallized from acetone and acetone–CH_2Cl_2 solutions as acetone solvates (structures **1B**, **2A** and **2B**), which were only poorly soluble in acetone. Interestingly, **2A** and **2B** formed simultaneously in the same test tube and are conformational polymorphs of each other.§ Structure **2A** was obtained from a plate and structure **2B** from a needle shaped crystal. Obtaining several polymorphs simultaneously under the same crystallization conditions is quite rare; an example of such a macrocyclic compound is furanotribenzo-21-crown-7 in which the conformation of the macrocycle is however unchanged.[56] Crystallographic data of all structures are presented in Table 1.

The resorcinarene core of all octapodands is in a boat conformation since all phenolic hydroxyl groups are alkylated.[4] The angle of the upright resorcinol rings C1–C6 and C15–C20 against

‡ For some crystallization experiments the amorphous form of **1** and **2** was used.

§ The original crystallization was made from acetone–DCM by dissolving part of the sample in acetone and adding DCM until the sample was fully dissolved. Later on pure acetone and acetone–DCM 3 : 1 were used.

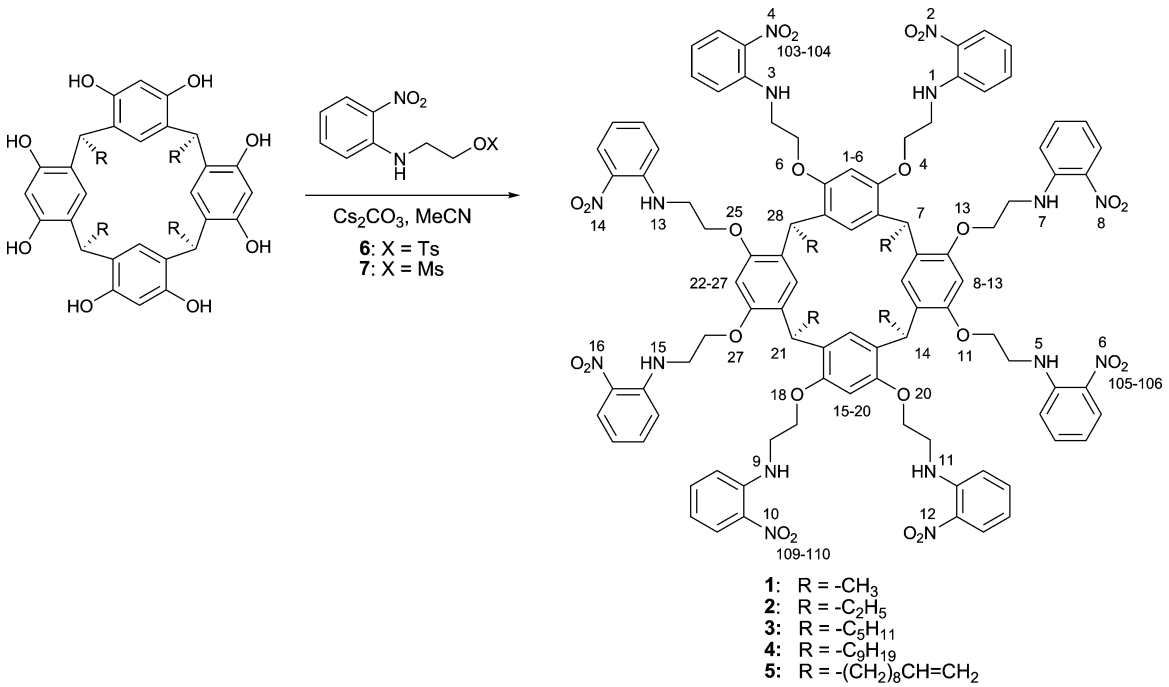

Scheme 1 Synthetic procedure and selected crystallographic numbering for octapodands.

Table 1 X-ray structure parameters

	1A	1B	2A	2B	2C	2D	5A
Crystallization solvent	nitromethane–CH_2Cl_2	acetone	acetone–CH_2Cl_2	acetone–CH_2Cl_2	nitromethane–CH_2Cl_2	acetonitrile–CH_2Cl_2	nitromethane–CH_2Cl_2
Crystal shape	block	plate	plate	needle	needle	block	rod
Crystal size/mm	0.40 × 0.20 × 0.20	0.20 × 0.12 × 0.08	0.18 × 0.14 × 0.02	0.20 × 0.08 × 0.02	0.24 × 0.10 × 0.04	0.20 × 0.10 × 0.10	0.20 × 0.10 × 0.10
Formula	$C_{96}H_{96}N_{16}O_{24}$	$C_{96}H_{96}N_{16}O_{24}\cdot(CH_3)_2CO$	$C_{100}H_{104}N_{16}O_{24}\cdot(CH_3)_2CO$	$C_{100}H_{104}N_{16}O_{24}\cdot(CH_3)_2CO$	$C_{100}H_{104}N_{16}O_{24}$[a]	$C_{100}H_{104}N_{16}O_{24}\cdot C_2H_3N$[a]	$C_{132}H_{160}N_{16}O_{24}\cdot 1.5H_2O$
FW	1857.89	1915.97	1972.07	1972.07	1913.99	1955.05	2381.78
a/Å	12.2700(3)	11.8003(4)	11.1398(3)	11.8347(3)	11.9965(3)	12.0137(3)	12.6739(5)
b/Å	19.6334(7)	20.6248(7)	22.0112(6)	20.5903(5)	20.2594(5)	20.2750(4)	20.5874(7)
c/Å	20.4221(6)	21.2868(8)	22.5117(6)	22.5132(7)	22.8564(5)	22.8339(4)	25.8506(9)
α (°)	75.230(2)	110.363(2)	113.189(2)	113.258(2)	114.695(1)	115.072(1)	77.841(3)
β (°)	72.675(2)	97.492(2)	100.427(2)	95.992(2)	96.9670(9)	96.578(1)	77.976(2)
γ (°)	75.364(2)	99.820(2)	99.965(1)	100.282(2)	99.770(2)	99.681(2)	74.025(2)
Volume/Å^3	4457.3(2)	4683.8(3)	4804.5(2)	4865.6(2)	4857.9(2)	4857.3(2)	6257.4(4)
D_c/Mg m^{-3}	1.384	1.359	1.363	1.346	1.308	1.337	1.264
μ/mm^{-1}	0.842	0.826	0.820	0.810	0.787	0.802	0.719
Meas. reflns	22810	23546	23754	21729	24568	23282	20941
Indep. reflns	15349	15426	16232	14853	16100	16813	14939
R_{int}	0.0584	0.0833	0.1092	0.1283	0.0743	0.0789	0.1675
R_1 [$I > 2\sigma(I)$]	0.0748	0.0824	0.0979	0.0935	0.0671	0.0651	0.1458
wR_2 [$I > 2\sigma(I)$]	0.2233	0.2008	0.2643	0.2192	0.1581	0.1754	0.3528
GooF on F^2	1.392	1.404	1.323	1.253	1.127	1.230	1.283

[a] Disordered solvent molecules were removed using SQUEEZE.[55]

Table 2 The upright resorcinol ring tilt angles against the C7–C14–C21–C28 plane

Structure	C1–C6 (°)	C15–C20 (°)
1A	76.2	87.1
1B	80.2	89.1
2A	84.4	88.3
2B	80.6	87.1
2C	81.2	86.7
2D	81.2	87.0
5A	100.1	97.6

the methine carbon plane C7–C14–C21–C28 varies between 76.2° and 87.1° in structure **1A** up to 100.1° and 97.6° in structure **5A** (Table 2), which is the only structure where both resorcinol rings are pointing slightly outwards opening the resorcinarene cavity. Structure **5A** differs from the other structures quite remarkably, since **5** is the only podand that has long 1-decenyl groups at the lower rim capable of packing next to each other due to van der Waals interactions. The packing of short alkyl chain podands **1** and **2** is directed by intermolecular hydrogen bonding of nitro and amine groups as well as π–π interactions between aromatic rings.

In general, the eight nitroaniline side arms at phenolic oxygens can be divided into two groups depending on whether they are bound to upright or horizontal resorcinol rings (Fig. 1): 'top' (O4, O6, O18 and O20, named after the oxygen atom they are attached to) which extend on top of the resorcinarene cavity and 'alongside' (O11, O13, O25 and O27) which point to the sides of the cavity. Most structures have their 'alongside' side arms in a vertical position but there is a little more variation in the 'top' side arm positions (see Table 3 for O–C–C–N distortion angles). In addition, podands form an upper rim interface where the resorcinarene cavities of two molecules approach each other, and tail-to-tail interface, where alkyl chains of the podands face each other.

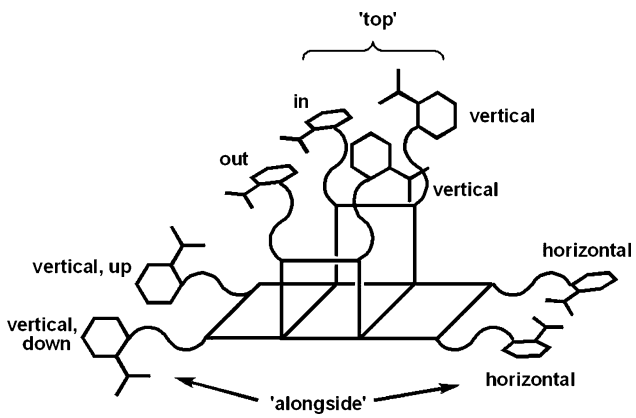

Fig. 1 Different orientations of the 'top' and 'alongside' side arms. The horizontal conformation of 'top' side arms is either 'in' or 'out' of the resorcinarene cavity.

Structure **1A** has three 'top' side arms in horizontal orientation (O4, O6 and O18), where side arms O4 and O6 form an intermolecular π-stack at the upper rim interface (Fig. 2). The remaining side arm O20 forms additional π-stacking with the resorcinol ring (C1–C6) not observed in other structures. Two of the 'alongside' side arms, O25 and O27 have twisted vertical conformations with distortion angles 73.6° and –67.4°, respectively, and they form intermolecular edge-to-face π-interactions between two parallel molecules. In addition, the side arm O25 approaches the resorcinol ring (C8–C13) forming another edge-to-face π-interaction at the tail-to-tail interface. Side arm O13 is horizontally oriented forming a π-stack with side arm O18 of the neighboring parallel molecule. Side arm O11, however, is between a horizontal and a vertical conformation forming an edge-to-face π-interaction with C22–C27 resorcinol ring of another molecule at the tail-to-tail interface, which explains the twisted conformation of the side arm O11.

Table 3 O–C–C–N distortion angles of the side arms

Structure	O4···N1	O6···N3	O11···N5	O13···N7	O18···N9	O20···N11	O25···N13	O27···N15
1A	55.3(4)	−52.1(4)	84.1(4)	−42.0(8)	74.5(4)	171.3(3)	73.6(3)	−67.4(3)
1B	−64.4(5)	56.8(4)	178.8(3)	135.1(8)[a]	63.7(5)	−177.0(3)	150.0(5)[a]	−51.6(9)[a]
2A	−63.1(5)	−165.0(4)	−175.7(4)	−174.5(4)	171.7(4)	−72.7(5)	173.2(5)	75.8(7)
2B	−62.8(6)	68.9(6)	−176.0(5)	152.1(6)[a]	61.0(7)	178.9(4)	−156.9(6)	173.2(4)
2C	61.5(4)	−66.2(3)	168.3(3)	−170.4(3)	−63.4(4)	−176.2(3)	156.2(4)	−179.2(3)
2D	60.4(4)	−66.3(3)	168.3(3)	−171.0(3)	−62.8(4)	−176.9(2)	160.1(3)	178.6(2)
5A	−66.1(10)	70.9(10)	164.0(11)	176.9(8)	76.3(9)	−74.3(10)	−168.3(15)[a]	−170.3(9)

[a] For disordered side arms the distortion angle for the part with higher site occupancy is reported.

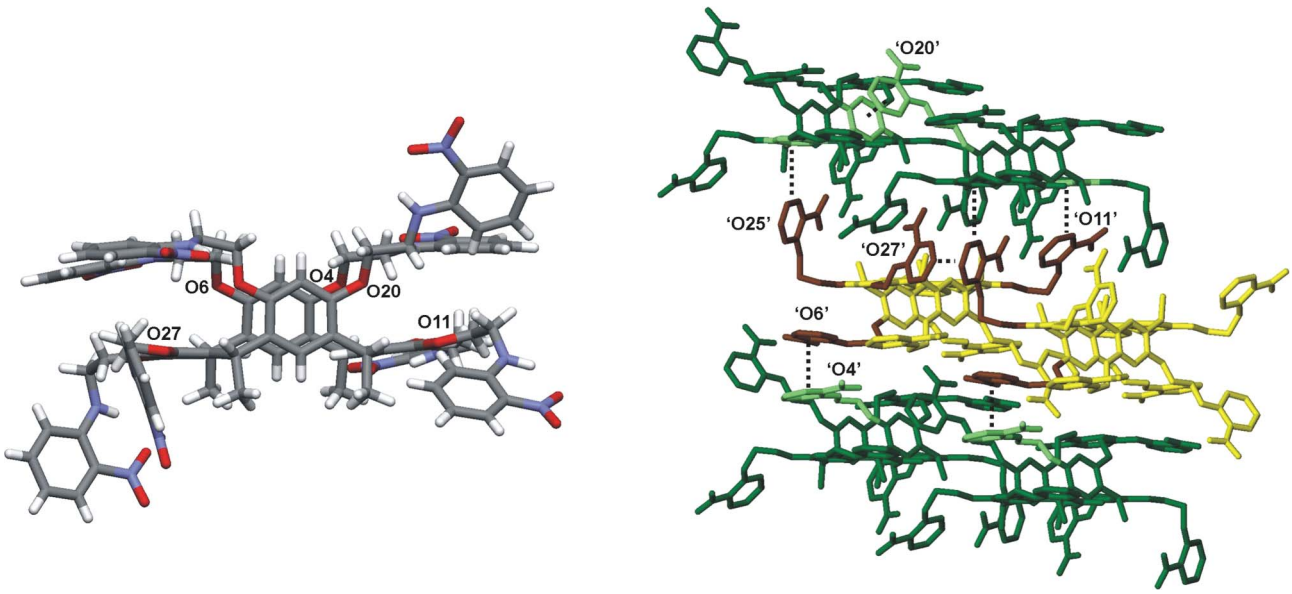

Fig. 2 Structure **1A** (side view) and packing illustrating π–π-interactions between side arms 'O4' and 'O6', 'O11' and C22–27, 'O20' and C1–C6, 'O25' and 'O27' as well as 'O25' and C8–13. π-stacking between side arms 'O13' and 'O18' is not shown.

Altogether, the π–π interactions of **1A** lead to a network like packing instead of rows of parallel molecules found in all other structures.

Acetone solvate **1B** crystallized from acetone providing beautiful block shaped crystals of relatively good quality. **1B** has an isomorphous unit cell and closely related structure to acetone solvate **2B**, structure **2C** and acetonitrile solvate **2D**. All of them can be characterized by rows of molecules joined together by π-stacks of four 'alongside' side arms (Fig. 3). Rows of podands pack next to each other forming an edge-to-face π-interaction between side arms O18 and O4. At the upper rim interface, rows are shifted with respect to each other, and connect through intertwined side arms O20 penetrating into the neighboring resorcinarene cavity (edge-to-face interaction with side arm O18), as well as O4···O4 π-stacking with another podand. At the tail-to-tail interface intermolecular hydrogen bonds between side arms O11 (nitro and amine groups) of nearby molecules connect two layers.

In structure **2B**, an acetone molecule is hydrogen bonded into N–H (N15) group whereas in **1B** the acetone molecule is simply positioned between the side arms O4 and O6 on top of the cavity. In **2A**, which is a conformational polymorph of **2B**, an acetone molecule is hydrogen bonded into N5, and rows of podands pack next to each other forming a more pronounced step like pattern with intermolecular π-interactions between side arms O4 and O20 (Fig. 3). The upper rim interface of **2A** is held together by intermolecular hydrogen bonding between side arms O6 and side arms O18 and O27 (N3–O103 and N15–O109) instead of pairing through side arms O20 (Fig. 4).

Structure **5A** with pendant 1-decenyl groups at the lower rim has a very symmetrical arrangement of the side arms with similar π-stacking of four 'alongside' side arms as structures **1B** and **2B–D**. In addition, the 'top' side arms are folded horizontally on top of the cavity, where each podand finds a pair in the facing row of podands through π–π-interactions of side arms O4 with O18, and O6 with O20. The facing rows of podands pack next to each other forming almost continuous layers of aromatic and aliphatic components through the crystal (Fig. 5) and since the aromatic part contains hydrophilic nitroaniline groups, compound **5** could present amphiphilic properties.

An indication of the versatile possibilities for these molecules to pack in the solid state is yet another structure of **1** obtained from the same crystallization experiment as structure **1A** containing a disordered solvent molecule. The data completeness was too low to provide decent temperature factors, but nevertheless, a different unit cell¶ and packing motif were confirmed, where all side arms

¶ $a = 14.6212(7)$ Å, $b = 16.7373(7)$ Å, $c = 19.5562(10)$ Å, $\alpha = 75.57(3)°$, $\beta = 89.870(2)°$, $\gamma = 87.986(3)°$, $V = 4631.9(4)$ Å^3

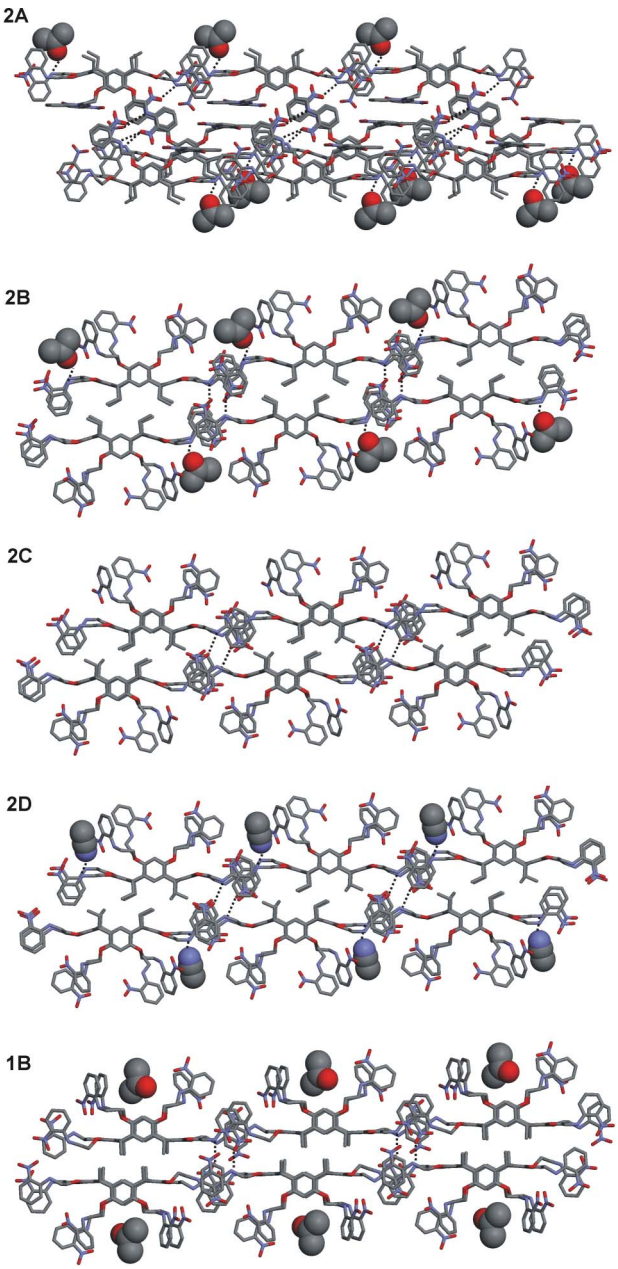

Fig. 3 Packing of structures **2A** (top), **2B**, **2C**, **2D** and **1B** (bottom) showing intermolecular hydrogen bonding (donor–acceptor) and omitting hydrogen atoms; solvent molecules are shown as CPK models except for structure **2C**, in which solvent molecules were removed by SQUEEZE.

have a vertical arrangement and podands are arranged in rows as in acetone solvate **1B** but where the upper rim interface is connected by intermolecular hydrogen bonding as in acetone solvate **2A**.

Powder X-ray diffraction

To elucidate the polymorphism and relative stability of the acetone solvates **2A** (plate) and **2B** (needle) powder X-ray diffraction experiments were carried out. Compound **2** was crystallized several times from acetone varying the crystallization speed and temperature. Fast crystallizations were conducted at room temperature by letting acetone evaporate overnight, which provided microcrystalline products. Slow crystallization was performed at 4 °C and crystals were filtered and dried briefly under vacuum. The X-ray diffraction patterns were compared with the calculated patterns of structures **2A** and **2B** showing that fast crystallization produced more structure **2A** and slow crystallization more structure **2B** (Fig. 6).‖ In addition, when acetone was removed rapidly under vacuum, only amorphous product was obtained indicating that crystallization process does not occur instantaneously.

When samples were placed under vacuum for more extended period, their diffraction pattern changed due to the loss of acetone and resulting changes in the lattice. After drying, unit cell parameters for a plate and a needle were collected and the plate matched still with the unit cell of **2A** but the parameters for a needle did not match either **2A** or **2B**, which indicates that structure **2A** might be more durable against collapse of the lattice when acetone is removed since its upper rim interface is hydrogen bonded. Based on these observations it seems that structure **2A** forms faster than **2B** when the system has more thermal energy (higher T), but both **2A** and **2B** are stable at room temperature and 4 °C, as well as –100 °C where single crystal data were collected. However, visual observation of the microcrystalline samples showed that they all contained both plates and needles, and the amount of plates and needles did not correspond to the ratio of **2A** and **2B** in the powder diffraction pattern.

Amphiphilic properties

The structural mobility and amphiphilic properties of the resorcinarene octapodands in solution were examined using NMR spectroscopy and Langmuir monolayer studies. Broad ^{1}H NMR resonances of **5** in $CDCl_3$ indicate that conformational changes occur approximately at the NMR timescale. Cooling to sub-zero temperatures slowed the movement below the NMR timescale where individual conformers could be observed as separate resonances appearing in the spectrum. Heating the sample to 60 °C, on the other hand, accelerated the movement which was observed as sharpening of individual resonances as well as improved resolution.

Interestingly, the rate of the conformational change could be adjusted by dissolving **5** in a more polar solvent, such as [D_6]acetone, in which sufficient resolution could be obtained at 30 °C (Fig. 7). In [D_6]DMSO the effect was even more profound. The behavior where polar solvent increases the mobility of polar parts of the molecule is known for amphiphiles,[57,58] and is expected to cause the observed changes for the octapodands as well.

For **3** and **4** the polarity of the solvent had a similar effect in the ^{1}H resonances whereas for **2** the effect was not as clear. Podand **1**, which contains short methyl groups at the lower rim, showed separate ^{1}H resonances for upright and horizontal resorcinol rings at 30 °C indicating slower boat-to-boat interconversion than for other podands. At –30 °C all nitroaniline protons except a proton *ortho* to the -NH group appear as two separate patterns in the spectrum and belong either to the upright or horizontal resorcinol ring according to ^{1}H, ^{1}H COSY and NOE spectra. NMR spectra are given in the ESI.†

Amphiphilicity of the podands **3–5** was confirmed by recording isotherms for monolayers of the podands on water, whereas **2** did

‖ Since powder X-ray patterns were measured at ambient temperature and single crystal data at 173 K, it should be noted that comparison between them has some limitations.

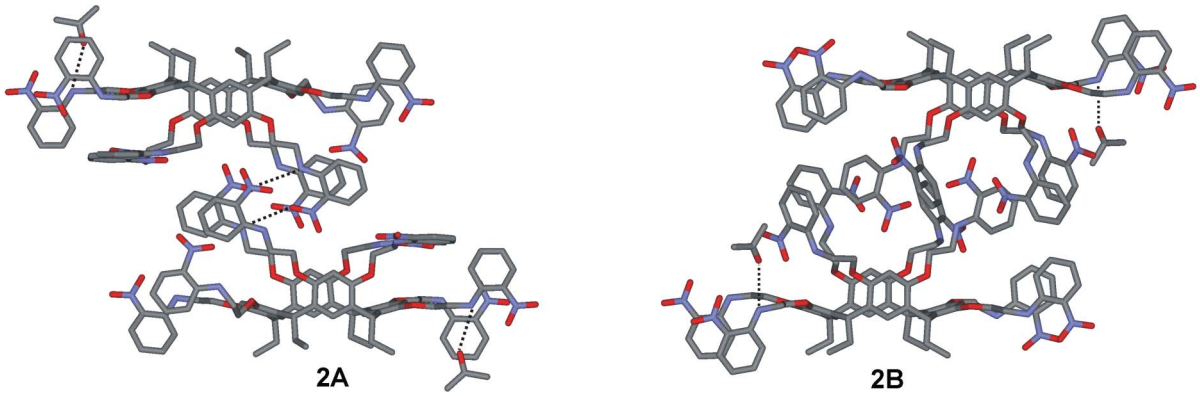

Fig. 4 Comparison of polymorphs **2A** and **2B**; intramolecular hydrogen bonds are shown with dashed lines (donor–acceptor), hydrogens are omitted for clarity.

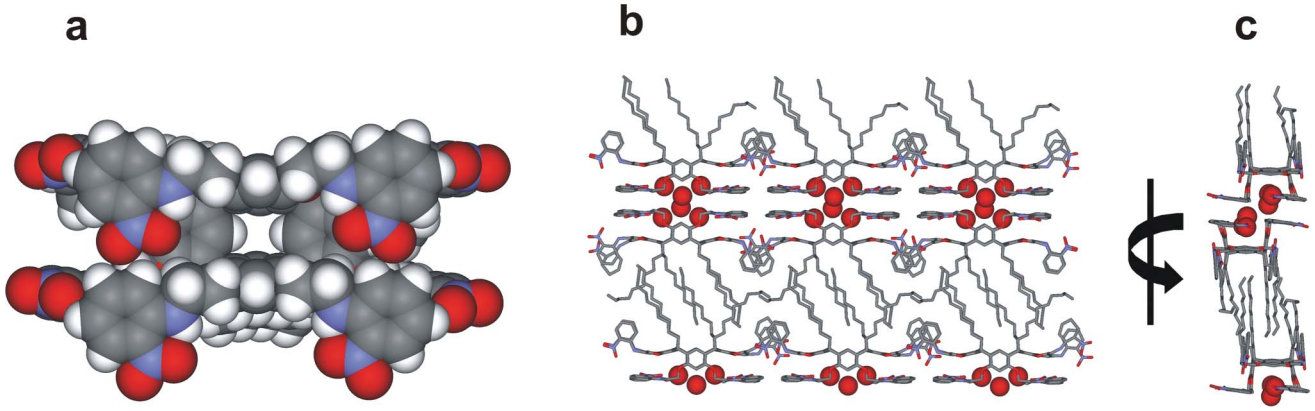

Fig. 5 Structure **5A** top view as a CPK model (a), solvent molecules are omitted for clarity. Packing (omitting hydrogens) viewed perpendicular to the plane of rows of podands (b), 90° rotation counterclockwise (c) illustrating π-interactions between pairs of podands. H_2O is shown as a CPK model and disorder is not shown for clarity.

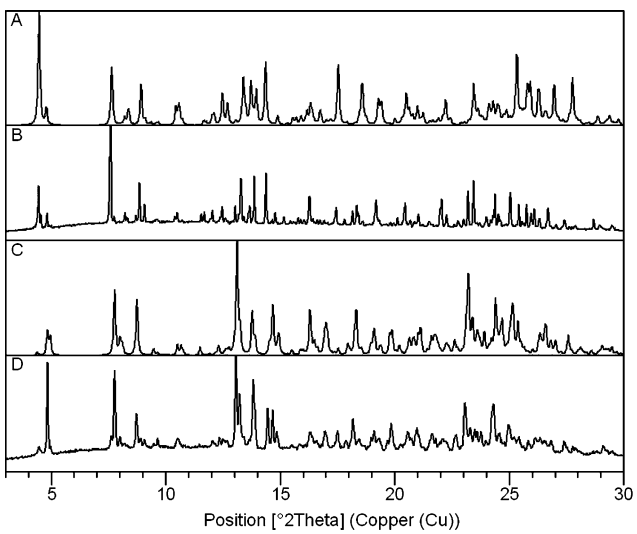

Fig. 6 Powder X-ray diffraction patterns (A) **2A** calculated structure, (B) fast crystallization of **2** at RT (C) **2B** calculated structure, (D) slow crystallization of **2** at 4 °C.

not form a monolayer on water due to the short ethyl chains at the lower rim. Compounds **3** and **4** formed monomolecular layers showing an increase in the collapse pressure from 8.6 to 18.2 mN m^{-1} with increasing chain length but monolayers of compound **5** collapsed at 12.8 mN m^{-1} which is probably caused by the disruption of terminal double bond to the aliphatic layer (Fig. 8). Collapse areas varied between 157 and 191 Å^2/molecule (Table 4), which are consistent when compared with the solid state structures (~170–250 Å^2). The relatively low collapse pressures recorded for these three octapodands can be interpreted as a consequence of the high flexibility of their polar head group preventing the amphiphiles from packing in a two dimensional interfacial solid phase. For compound **4** unexpected behaviour was observed in further studies with different alkali and earth alkali metal salts dissolved in the subphase since the collapse area showed quite large variation when recorded on subsequent days in water. A possible

Table 4 Isotherm parameters of the monolayers, areas are given as Å^2/molecule. A_{lim} is the extrapolation of the linear part of the isotherm on the *x* axis, A_0 and A_1 represent apparent molecular areas for surface tensions at 0 and 1 mN m^{-1} respectively

	3	**4**	**5**
collapse pressure/mN m^{-1}	8.6	18.2	12.8
collapse area/Å^2	191	157	166
A_{lim}/Å^2	221	187	197
A_0/Å^2	227	200	210
A_1/Å^2	219	192	201

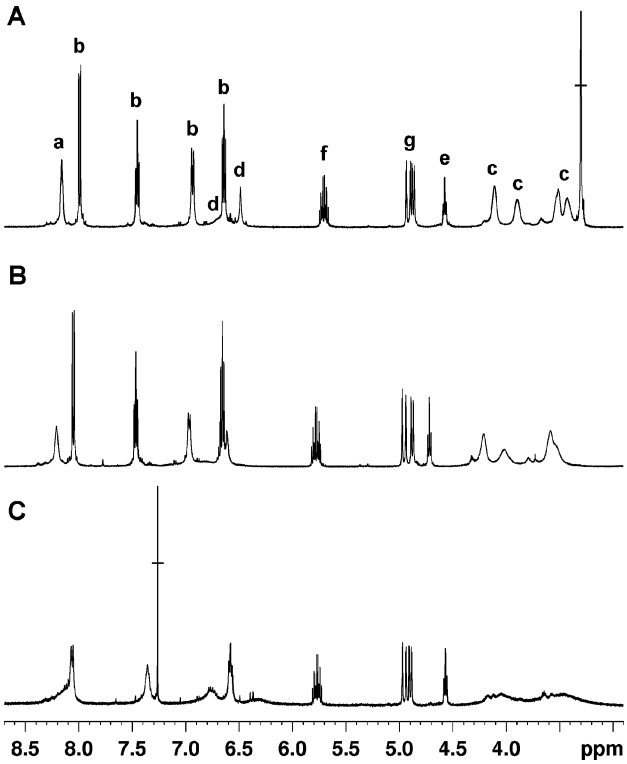

Fig. 7 ^{1}H NMR spectra of **5** in (A) [D6]DMSO, (B) [D6]acetone and (C) $CDCl_3$; resonances at 2.9–8.7 ppm, a: N*H*, b: nitroaniline Ar*H*, c: OCH_2CH_2N, d: resorcinarene core Ar*H*, e: Ar*CH*, f: alkyl tail *CH*=CH_2, g: alkyl tail CH=CH_2.

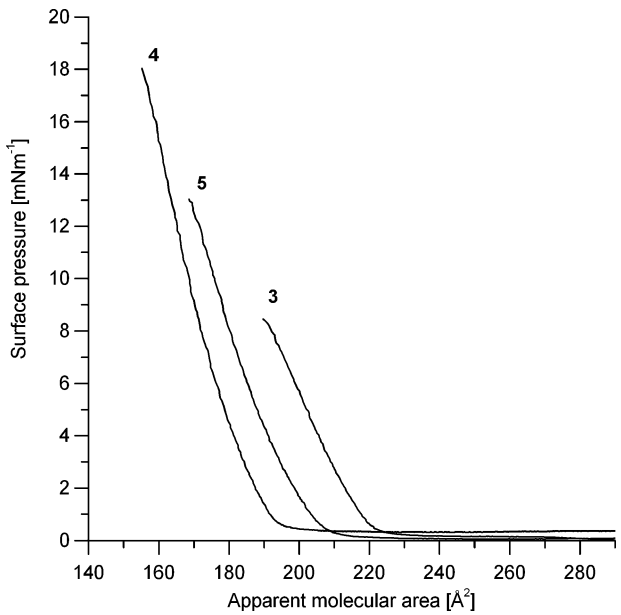

Fig. 8 Isotherms of podands **3**, **4** and **5**.

explanation could be found from the structural properties of the compound, since different conformations of the polar and flexible upper rim might lead to different packing also at the air–water interface. However, further experiments are required to confirm these preliminary observations.

Conclusions

Resorcinarene octapodands **1–5** exhibit versatile self-assembling properties, and show high conformational mobility due to boat-to-boat interconversion as well as the rotation around upper rim side arm -OCH_2CH_2N- linkers. Structural mobility is observed in the solid state as conformational polymorphism of **2**, and as disordered side arms and large temperature factors for nitroaniline groups. The different packing motifs observed for compounds **1** and **2** suggests that there are more than one almost equally favorable conformations in the solid state, probably depending on whether π–π-interactions or H-bonds form first during the crystallization process. The ratio of polymorphs **2A** and **2B** can be controlled by changing crystallization conditions, namely temperature and speed of solvent evaporation, which indicates that these molecules approach the limit where further structural flexibility leads to random precipitation instead of organized crystal structures. The X-ray diffraction data obtained for **2A** and **2B** also implies that **2A** with more extensive hydrogen bonding at the upper rim might be more stable against collapsing when acetone is removed from the lattice.

Compound **5** formed crystals from nitromethane–CH_2Cl_2 with continuous aliphatic and aromatic layers, where aliphatic groups of the molecule as well as π-interactions between side arms control the crystallization process. The conformational mobility, which leads to polymorphism and versatile conformations of the side arms observed in all crystal structures was further demonstrated in solution by ^{1}H NMR, where long chain octapodands **3–5** showed remarkable conformational flexibility and amphiphilic properties, which were confirmed by forming Langmuir monolayers. In contrast to the solid state structures, where the binding cavity of resorcinarenes was quite often blocked by side arms, conformational mobility of boat-to-boat interconversion and side arm rotation could lead to successive opening and closing of the binding cavity of the podands in solution. NMR spectra recorded in various solvents and temperatures showed how the energetics of these events can be tuned when the lower rim substituents are changed from methyl to ethyl or to longer alkyl chains.

Conformational polymorphism of resorcinarenes and other macrocyclic compounds has remained largely unexplored even though the importance of new polymorphs can be easily observed in the field of host–guest chemistry. Further chemical modification of the investigated podands could provide a variety of host molecules in which the binding properties in the solid state could be tuned by changing crystallization conditions. In addition, the amphiphilicity could be utilized in preparing self-assembling structures, such as monolayers, vesicles or micellar structures with novel binding properties.

Experimental Methods

General

All chemicals and solvents were purchased from Sigma–Aldrich and they were used as received. Acetonitrile was dried with $CaCl_2$ and distilled over molecular sieves. NMR spectra were recorded with a Bruker Avance DRX (500 MHz for ^{1}H and 126 MHz for ^{13}C) spectrometer at 30 °C unless otherwise stated. *J* values are given in Hz. ESI-MS spectra were measured with a Micromass

LCT (ESI-TOF) instrument. Melting points were determined with a Metler Toledo FP62 apparatus and are uncorrected. Elemental analyses were performed on a Vario EL III apparatus. Thermogravimetric/differential thermal analysis was measured with a Perkin Elmer Diamond TG/DTA. Samples were placed in a platinum sample pan and measured with a temperature program 25–900 °C at 10 °C min^{-1}.

General procedure for resorcinarene octapodands

Resorcinarene, dibenzo-18-crown-6 (0.16 molar equivalents) and dry Cs_2CO_3 or K_2CO_3 (16 molar equivalents) were suspended in dry acetonitrile under nitrogen atmosphere and refluxed for 15 min followed by an addition of 8 molar equivalents of **6**[54] or **7** in acetonitrile. The yellow suspension was refluxed for 24 h, filtered with suction and evaporated under reduced pressure. The residue was suspended in water and extracted with dichloromethane; organic layer was dried over $MgSO_4$ and evaporated to dryness. The product was purified with flash chromatography (SiO_2; $CHCl_3$–MeOH), dissolved in acetone and precipitated from water with an addition of NaCl, or recrystallized from acetone. The product was filtered with suction and dried under vacuum. Detailed synthetic procedure for each podand along with spectroscopic data is provided in the ESI.†

o-Nitro-*N*-(2-methanesulfonyloxyethyl)aniline 7

o-Nitro-*N*-(2-hydroxyethyl)-aniline[59,60] (2.74 g, 15.0 mmol) was dissolved in 5 ml of pyridine under nitrogen atmosphere and cooled in an ice bath. Methanesulfonylchloride (1.4 ml, 18.1 mmol) was added drop wise into the solution. After mixing one hour in an ice bath and one hour in the room temperature, reaction was quenched by adding 50 ml of water. The orange crystals were filtered with suction, washed with water and dried under vacuum. The product was recrystallized from hot chloroform–hexane, filtered and dried under vacuum to afford yellow–orange crystals (3.0 g, 76%). mp 82–83 °C; (Found: C, 41.55; H, 4.5; N, 10.8. $C_9H_{12}N_2O_5S$ requires C, 41.5; H, 4.65; N, 10.8%); δ_H(500 MHz, $CDCl_3$) 3.05 (s, 3H; CH_3), 3.73 (q, ^3J (H,H) = 5.7, 2H; NCH_2), 4.46 (t, ^3J (H,H) = 5.6, 2H; OCH_2), 6.73 (m, 1H; Ar*H*), 6.89 (dd, ^3J (H,H) = 8.6, ^4J (H,H) = 0.9, 1H; Ar*H*), 7.48 (m, 1H; Ar*H*), 8.18 (br, 1H; N*H*), 8.20 (dd, ^3J (H,H) = 8.6, ^4J (H,H) = 1.6, 1H; Ar*H*); δ_C(126 MHz, $CDCl_3$) 37.9 (CH_3), 42.1 (NCH_2), 66.8 (OCH_2), 113.5 (*Ar*H), 116.5 (*Ar*H), 127.3 (*Ar*H), 133.0 ($ArNO_2$), 136.6 (*Ar*H), 144.7 (*Ar*NH); *m*/*z* (ESI-TOF) 283 (M + Na^+, 100%) 261 (M + H^+, 8), 187 (60), 165 ($M^+ - SO_3CH_3$, 38).

X-Ray crystallography

Powder X-ray diffraction patterns were measured on a PANalytical X'Pert Pro system in reflection mode using monochromatized Cu-Kα radiation (λ = 1.54178 Å) at ambient temperature. The 2θ angle range was 3–30°.

Single crystal X-ray data were recorded on a Nonius Kappa CCD diffractometer with Apex II detector using graphite monochromatized Cu-Kα [λ = 1.54178 Å] radiation at a temperature of 173 K. The data were processed and absorption correction was made to all structures with Denzo-SMN v0.97.638.[61] The structures were solved by direct methods (SHELXS-97) and refined (SHELXL-97) against F^2 by full-matrix least-squares techniques using SHELX-97 software package.[62] The hydrogen atoms were calculated to their idealized positions with isotropic temperature factors (1.2 or 1.5 times the C temperature factor) and refined as riding atoms unless otherwise mentioned. All compounds crystallized as triclinic $P\bar{1}$ with Z = 2. Crystal structure analysis was done using Mercury CSD 2.3 software.[63] Crystallographic data (excluding structure factors) for the structures in this paper have been deposited with the Cambridge Structural Data Center as supplementary publication nos. CCDC 781919–781925.† Copies of the data can be obtained free of charge from The Cambridge Crystallographic Data Centre *via* www.ccdc.cam.ac.uk/data_request/cif.

Langmuir monolayer studies

Langmuir isotherms were recorded using a 112D Nima Technology (Coventry, U.K.) system. Spreading solutions were prepared by dissolving **2–5** in chloroform at 2 mg ml^{-1} concentration and diluted to 0.5 mg ml^{-1} by weighing the amount of solvent. Monolayers were prepared on purified water (Millipore Milli-Q water system, resistivity ≥18 MΩ·cm) by adding 20 µl of spreading solution on the surface and recording the isotherm after 15 min with compression rate set at 5 cm^2 min^{-1} from 85 to 14 cm^2 or until a collapse point was observed. Each isotherm was recorded at least three times to ensure the reliability of the results.

Acknowledgements

This work was financially supported by Academy of Finland (projects 117945 and 116503) and National Graduate School of Organic Chemistry and Chemical Biology. We are grateful to Mr Reijo Kauppinen for his help with the NMR studies.

Notes and references

1 J. Vicens and V. Böhmer, *Topics in Inclusion Science, Vol. 3: Calixarenes: A Versatile Class of Macrocyclic Compounds*, Kluwer Academic Publishers, Netherlands, 1991, pp.264.
2 L. Mandolini and R. Ungaro, *Calixarenes in Action*, Imperial College Press, Singapore, 2000, pp.271.
3 C. D. Gutsche, *Calixarenes Revisited*, The Royal Society of Chemistry, UK, 1998, pp. 233.
4 P. Timmerman, W. Verboom and D. N. Reinhoudt, *Tetrahedron*, 1996, **52**, 2663–2704.
5 S. M. Biros and J. Rebek Jr, *Chem. Soc. Rev.*, 2007, **36**, 93–104.
6 W. Sliwa and C. Kozlowski, *Calixarenes and resorcinarenes*, Wiley-VCH, Germany, 2009, pp. 316.
7 Y. Liu, H. Wang, L. Wang, Z. Li, H. Zhang and Q. Zhang, *Tetrahedron*, 2003, **59**, 7967–7972.
8 M. M. Reinoso García, W. Verboom, D. N. Reinhoudt, E. Malinowska, M. Pietrzak and D. Wojciechowska, *Tetrahedron*, 2004, **60**, 11299–11306.
9 M. A. Sarmentero and P. Ballester, *Org. Biomol. Chem.*, 2007, **5**, 3046–3054.
10 U. Darbost, M. Rager, S. Petit, I. Jabin and O. Reinaud, *J. Am. Chem. Soc.*, 2005, **127**, 8517–8525.
11 S. Busi, H. Saxell, R. Fröhlich and K. Rissanen, *CrystEngComm*, 2008, **10**, 1803–1809.
12 H. Mansikkamäki, M. Nissinen and K. Rissanen, *CrystEngComm*, 2005, **7**, 519–526.
13 A. J. McConnell, C. J. Serpell, A. L. Thompson, D. R. Allan and P. D. Beer, *Chem.–Eur. J.*, 2010, **16**, 1256–1264.
14 M. H. Filby, T. D. Humphries, D. R. Turner, R. Kataky, J. Kruusma and J. W. Steed, *Chem. Commun.*, 2006, 156–158.
15 S. Le, Gac and I. Jabin, *Chem.–Eur. J.*, 2008, **14**, 548–557.
16 M. Ménand and I. Jabin, *Chem.–Eur. J.*, 2010, **16**, 2159–2169.

17 F. Perret, A. N. Lazar and A. W. Coleman, *Chem. Commun.*, 2006, 2425–2438.
18 A. W. Coleman, F. Perret, A. Moussa, M. Dupin, Y. Guo and H. Perron, *Top. Curr. Chem.*, 2007, **277**, 31–88.
19 Y. Sun, C. Yan, Y. Yao, Y. Han and M. Shen, *Adv. Funct. Mater.*, 2008, **18**, 3981–3990.
20 Y. Sun, Y. Yao, C. Yan, Y. Han and M. Shen, *ACS Nano*, 2010, **4**, 2129–2141.
21 B. Kim, S. L. Tripp and A. Wei, *J. Am. Chem. Soc.*, 2001, **123**, 7955–7956.
22 A. Wei, B. Kim, S. V. Pusztay, S. L. Tripp and R. Balasubramanian, *J. Inclusion Phenom. Macrocyclic Chem.*, 2001, **41**, 83–86.
23 A. Wei, *Chem. Commun.*, 2006, 1581–1591.
24 J. Liu and A. Wei, *Chem. Commun.*, 2009, 4254–4256.
25 H. Kitagawa, M. Kawahata, R. Kitagawa, Y. Yamada, M. Yamanaka, K. Yamaguchi and K. Kobayashi, *Tetrahedron*, 2009, **65**, 7234–7239.
26 A. W. Coleman, S. Jebors, P. Shahgaldian, G. S. Ananchenko and J. A. Ripmeester, *Chem. Commun.*, 2008, 2291–2303.
27 A. Shivanyuk, *J. Am. Chem. Soc.*, 2007, **129**, 14196–14199.
28 K. Helttunen and P. Shahgaldian, *New J. Chem.*, 2010, DOI: 10.1039/C0NJ00123F.
29 D. Volkmer, M. Fricke, D. Vollhardt and S. Siegel, *J. Chem. Soc., Dalton Trans.*, 2002, 4547–4554.
30 P. Shahgaldian, M. A. Sciotti and U. Pieles, *Langmuir*, 2008, **24**, 8522–8526.
31 L. Nault, A. Cumbo, R. F. Pretôt, M. A. Sciotti and P. Shahgaldian, *Chem. Commun.*, 2010, **46**, DOI: 10.1039/b926025k.
32 S. Ehrler, U. Pieles, A. Wirth-Heller and P. Shahgaldian, *Chem. Commun.*, 2007, 2605–2607.
33 H. Mansikkamäki, M. Nissinen and K. Rissanen, *Angew. Chem., Int. Ed.*, 2004, **43**, 1243–1246.
34 H. Mansikkamäki, S. Busi, M. Nissinen, A. Åhman and K. Rissanen, *Chem.–Eur. J.*, 2006, **12**, 4289–4296.
35 M. Makha, C. W. Evans, A. N. Sobolev and C. L. Raston, *Cryst. Growth Des.*, 2008, **8**, 2929–2932.
36 D. Sun and C. A. Reed, *Chem. Commun.*, 2000, 2391–2392.
37 B. Ma, Y. Zhang and P. Coppens, *J. Org. Chem.*, 2003, **68**, 9467–9472.
38 G. R. Desiraju, *Angew. Chem., Int. Ed.*, 2007, **46**, 8342–8356.
39 E. Nomura, M. Takagaki, C. Nakaoka and H. Taniguchi, *J. Org. Chem.*, 2000, **65**, 5932–5936.
40 T. Gruber, M. Peukert, D. Schindler, W. Seichter, E. Weber and P. Bombicz, *J. Inclusion Phenom. Macrocyclic Chem.*, 2008, **62**, 311–324.
41 P. Thuéry, M. Nierlich, R. Calemczuk, M. Saadioui, Z. Asfari and J. Vicens, *Acta Crystallogr., Sect. B: Struct. Sci.*, 1999, **B55**, 95–103.
42 J. L. Atwood, L. J. Barbour and A. Jerga, *Chem. Commun.*, 2002, 2952–2953.
43 S. H. Dale, M. R. J. Elsegood and C. Redshaw, *CrystEngComm*, 2003, **5**, 368–373.
44 A. Nangia, *Acc. Chem. Res.*, 2008, **41**, 595–604.
45 P. K. Thallapally, G. O. Lloyd, T. B. Wirsig, M. W. Bredenkamp, J. L. Atwood and L. J. Barbour, *Chem. Commun.*, 2005, 5272–5274.
46 J. L. Atwood, L. J. Barbour and A. Jerga, *Science*, 2002, **296**, 2367–2369.
47 J. L. Atwood, L. J. Barbour and A. Jerga, *Angew. Chem., Int. Ed.*, 2004, **43**, 2948–2950.
48 S. J. Dalgarno, J. Tian, J. E. Warren, T. E. Clark, M. Makha, C. L. Raston and J. L. Atwood, *Chem. Commun.*, 2007, 4848–4850.
49 J. L. Atwood, L. J. Barbour, P. K. Thallapally and T. B. Wirsig, *Chem. Commun.*, 2005, 51–53.
50 A. V. Yakimov, M. A. Ziganshin, A. T. Gubaidullin and V. V. Gorbatchuk, *Org. Biomol. Chem.*, 2008, **6**, 982–985.
51 K. Salorinne and M. Nissinen, *Org. Lett.*, 2006, **8**, 5473–5476.
52 K. Salorinne and M. Nissinen, *Tetrahedron*, 2008, **64**, 1798–1807.
53 K. Salorinne, T. Tero, K. Riikonen and M. Nissinen, *Org. Biomol. Chem.*, 2009, **7**, 4211–4217.
54 K. Salorinne, D. P. Weimann, C. A. Schalley and M. Nissinen, *Eur. J. Org. Chem.*, 2009, 6151–6159.
55 P. Van, der Sluis and A. L. Spek, *Acta Crystallogr., Sect. A: Found. Crystallogr.*, 1990, **A46**, 194–201.
56 J. H. Burns, J. C. Bryan, M. C. Davis and R. A. Sachleben, *J. Inclusion Phenom. Mol. Recognit. Chem.*, 1996, **26**, 197–207.
57 K. Miyazawa and F. M. Winnik, *Macromolecules*, 2002, **35**, 9536–9544.
58 T. Kai, X. Sun, K. M. Faucher, R. P. Apkarian and E. L. Chaikof, *J. Org. Chem.*, 2005, **70**, 2606–2615.
59 J. M. McManus and R. M. Herbst, *J. Org. Chem.*, 1959, **24**, 1042–1043.
60 L. Westerheide, F. K. Müller, R. Than, B. Krebs, J. Dietrich and S. Schindler, *Inorg. Chem.*, 2001, **40**, 1951–1961.
61 Z. Otwinowski and W. Minor, *Methods Enzymol.*, 1997, **276**, 307–326.
62 G. M. Sheldrick, *Acta Crystallogr., Sect. A: Found. Crystallogr.*, 2008, **A64**, 112–122.
63 C. F. Macrae, I. J. Bruno, J. A. Chisholm, P. R. Edgington, P. McCabe, E. Pidcock, L. Rodriguez-Monge, R. Taylor, J. van de Streek and P. A. Wood, *J. Appl. Crystallogr.*, 2008, **41**, 466–470.

